Available online at www.sciencedirect.com
SCIENCE DIRECT®
Polymer 45 (2004) 2281–2290
polymer
www.elsevier.com/locate/polymer

Solid-state ^{19}F MAS and $^{1}H \rightarrow {}^{19}F$ CP/MAS NMR study of the phase transition behavior of vinylidene fluoride–trifluoroethylene copolymers: 1. Uniaxially drawn films of VDF 75% copolymer

Keitaro Aimi[a], Shinji Ando[a,*], Paolo Avalle[b], Robin K. Harris[b]

[a]*Department of Organic and Polymeric Materials, Tokyo Institute of Technology, Ookayama, Meguro-ku, Tokyo 152-8552, Japan*
[b]*Department of Chemistry, University of Durham, South Road, Durham DH1 3LE, UK*

Received 10 October 2003; received in revised form 29 December 2003; accepted 8 January 2004

Abstract

The changes in the phase structures and molecular mobility caused by the ferroelectric–paraelectric phase transition of vinylidene fluoride (VDF) and trifluoroethylene (TrFE) copolymer, P(VDF_{75}/$TrFE_{25}$), were analyzed using variable temperature (VT) solid-state ^{19}F MAS and $^{1}H \rightarrow {}^{19}F$ CP/MAS NMR spectroscopy. The CF_2 signal of the VDF chain sequence and the CHF signal at the *head*-to-*head* linkage of VDF–TrFE sequence showed higher frequency shift in the temperature range 43–92 °C, whereas no change was found for the CHF signal at the *head*-to-*tail* linkage of VDF–TrFE up to 92 °C. Hence, VT ^{19}F MAS spectra revealed that the VDF–TrFE *head*-to-*tail* sequence is the most stable part in polymer chains against *trans*–*gauche* conformational exchange motions below the phase transition temperature (Curie temperature, T_c) on heating. However, all chain sequences including TrFE units undergo conformational exchange at around T_c. The phase transition behavior is clearly recognized in the ^{19}F spectral shapes, in which the broad signals of the ferroelectric immobile phase disappeared between 115 and 119 °C. In addition, $T_{1\rho}^{F}$ for all peaks decreased to a unique value (ca. 20 ms) at 119 °C, indicating that uniform molecular motion accompanied by a full chain rotation occurred at the temperature. The significantly longer $T_{1\rho}^{F}$ for all peaks (ca. 20 ms) in the paraelectric phase (119 °C) than that in the amorphous domain (<4 ms) at ambient temperature supports the conclusion that there is restricted rotational motion of polymer chains around the chain axis in the paraelectric phase. On cooling from 119 to 85 °C, a gradual decrease in *gauche* conformers in the paraelectric phase was confirmed by the low-frequency displacement of CF_2 signals in VDF sequences accompanied by slight decreases in T_1^F and $T_{1\rho}^{F}$. The phase transition was observed between 85 and 77 °C on cooling, in which the characteristic signals of the paraelectric phase disappeared, the $T_{1\rho}^{F}$ values of all peaks quickly increased, and the broad crystalline signals abruptly appeared at 77 °C.

Keywords: Vinylidene fluoride–trifluoroethylene copolymers; Phase transition; ^{19}F MAS NMR

1. Introduction

Vinylidene fluoride (VDF) and trifluoroethylene (TrFE) copolymers (P(VDF/TrFE)) are known to exhibit piezoelectric and pyroelectric properties, and they have attracted much interest for their ferroelectric-to-paraelectric phase transition phenomena [1,2]. In particular, Ohigashi et al. [3] have found that a highly double-oriented film can be obtained from an uniaxially drawn film of P(VDF/TrFE) by crystallization in the paraelectric phase with its surfaces free from any constraint other than the tensile stress in the stretched direction. They called the drawn film 'single crystalline (SC) film' since neither amorphous regions nor lamellar structures were detected by X-ray diffraction. The crystal structures, thermal behavior, and piezoelectric properties of the copolymer depend on the VDF contents of P(VDF_x/$TrFE_{1-x}$). A high piezoelectric property is developed when the VDF content (x) is 0.65–0.82. Many studies have been reported to clarify the phase transition behavior of P(VDF/TrFE) by infrared spectra [4], X-ray diffraction [5,6], molecular dynamics calculations [7], and ^{1}H and ^{13}C NMR spectroscopy [8–11]. In the low-temperature (ferroelectric) phase, the stable crystal structure is orthorhombic, in which all-*trans* chains pack with their electric dipoles oriented in parallel along the *b* axis. In the high-temperature (paraelectric) phase, the crystal structure is hexagonal, formed with statistically mixed chains of

* Corresponding author. Tel.: +81-3-5734-2137; fax: +81-3-5734-2889.
E-mail address: sando@polymer.titech.ac.jp (S. Ando).

0032-3861/$ - see front matter © 2004 Published by Elsevier Ltd.
doi:10.1016/j.polymer.2004.01.005

TG^+, TG^-, T_3G^+ and T_3G^-, and it has been proposed that the chains rotate around the chain axis with one-dimensional diffusion motion of the conformational defects along the chain [2,4,5,12].

Several NMR studies have been reported for analyses of molecular dynamics and phase-transition behavior of P(VDF/TrFE). Using ^{1}H NMR relaxation parameters, Ishii et al. [8–10] have proposed that the motional mode of the *trans* TrFE segments in the ferroelectric phase changes from a flip-flop motion to a hindered rotation near the phase-transition temperature (Curie temperature, T_c) on heating. They suggested that the vigorous motion of TrFE units may play a key role for the conformational change from all-*trans* to statistically mixed conformations during the phase transition. They also showed that the ^{1}H spin–lattice relaxation times in the rotating frame, $T_{1\rho}^H$, obtained from ^{13}C CP/MAS NMR measurements, exhibit minimal values in three temperature regimes, i.e. near T_c on heating (110 °C) and cooling (80 °C), and in the paraelectric phase on cooling (120–110 °C) [11].

High-resolution solid-state NMR allows us to analyze in detail the chemical structure, conformation, and molecular motion of fluoropolymers at the atomic level. In particular, solid-state ^{19}F MAS NMR has unique advantages due to the high natural abundance (100%) and the wide chemical shift range (>200 ppm) [13,14]. The ^{19}F MAS NMR technique has been applied to poly(vinylidene fluoride) (PVDF), poly(trifluoroethylene) (PTrFE), poly(vinylfluoride) (PVF), a copolymer of VDF and hexafluoropropyrene, and amorphous perfluoropolymers [15–22]. In addition, broad-band ^{1}H decoupling has been applied to the polymers containing protons. In this article, we examine the changes in the molecular conformation and molecular mobility at the VDF and TrFE moieties of P(VDF_{75}/$TrFE_{25}$) 'single-crystalline-like' films using variable temperature solid-state ^{19}F MAS and ^{1}H → ^{19}F CP/MAS NMR spectroscopy. As previously reported for PVDF [17], the signals for regio-irregular sequences are clearly distinguished from the regio-regular ones in the ^{19}F MAS spectra. In addition, the γ-*gauche* effect on ^{19}F chemical shifts (δ_F) of CF_2 causes a lower frequency shift of ca. 15 ppm, which is about three times larger than that on δ_C for CH_2 [17]. Hence, the ^{19}F NMR method allows us to analyze phase transition behaviors of polymers at the primary structure level. To our best knowledge, this is the first report on the phase-transition behaviors of fluoropolymers using the ^{19}F MAS NMR technique.

In addition, solid-state ^{1}H → ^{19}F CP/MAS NMR has a potential advantage for the analysis of phase structures and molecular dynamics of fluoropolymers that contain both fluorine and hydrogen atoms in their systems [18–20,24]. Although no improvement in sensitivity is expected for ^{19}F signals due to the high natural abundance of ^{19}F and ^{1}H, the CP experiments can provide selective observation of mobile or rigid phases, parameters related to ^{1}H → ^{19}F CP dynamics, effective inter-nuclear distances between fluorine and proton nuclei, and background-free spectra (generally NMR probes contain per fluorinated compounds).

2. Experimental

2.1. Samples

Poly(vinylidene fluoride–trifluoroethylene), P(VDF_{75}/-$TrFE_{25}$), film of commercial origin (as-received film, AR-film), supplied by Daikin Industries, Ltd, was used for this work. In addition, uniaxially drawn films of the copolymer were prepared by the following process [3]: Pellets of copolymer were dissolved in DMF with a concentration of 25 wt% and spin-coated onto a substrate. After drying at 70 °C for 3 h, the film was peeled off from the substrate and uniaxially drawn with a draw ratio of 5 at room temperature, followed by annealing at 140 °C for 3 h. The films obtained were 15 μm thick, colorless, and transparent. No scattering was observed, suggesting that the crystalline domains are much larger than the wavelengths of visible light. Hereafter, we denote these drawn films as SC-film.

2.2. DSC measurements

For determining phase transition temperatures, differential scanning calorimetory (DSC) was performed with a SEIKO SSS-5000 DSC-220 in the range 30–140 °C at a heating/cooling rate of 5 °C/min. Melting temperatures were measured by another DSC measurement at a heating rate of 10 °C/min.

2.3. Nuclear magnetic resonance

Solid-state NMR experiments were carried out on a JEOL EX spectrometer operating at resonance frequencies of 282.65 MHz for fluorine and 300.40 MHz for proton with a Chemagnetics APEX ^{19}F/^{1}H dual-tune probe and 4 mm o.d. zirconia Pencil rotors. Samples were spun at the magic angle at a rate of $\omega_r = 16$ kHz. The fluorine and proton r.f. fields were adjusted to fulfil the Hartmann–Hahn sideband matching condition, $\omega_{1H} = \omega_{1F} - \omega_r = 83$ kHz. Temperatures inside the rotor were calibrated using the ^{1}H chemical shifts of ethylene glycol absorbed on tetrakis(trimethylsilyl)silane spun at the same rate (16 kHz) [25]. The ambient probe temperature was estimated to be 68 °C. The temperatures were precisely controlled between 43 and 119 °C under VT measurement conditions. All NMR experiments were carried out under thermal equilibrium conditions at each temperature (signal acquisitions were started 15 min after setting of temperature). Fluorine chemical shifts are quoted with respect to the signal for $CFCl_3$ and were measured via replacement with a sample of liquid C_6F_6 (−163.6 ppm) with 83 kHz of proton decoupling field to correct the Bloch–Siegert effect [26]. Samples were packed at the center of the rotor with 2.5 mm thickness

along the axis direction to ensure homogeneity of the r.f. field and temperature. The number of acquisitions was 32 throughout the experiments except for delayed-CP operation.

Spin–lattice relaxation times in the rotating frame for ^{19}F ($T_{1\rho}^{F}$) were measured by variable spin-lock time experiments. The relevant pulse sequence is depicted in Fig. 1(a). The spin-lock time (t_{SL}) was varied from 0.01 to 20 ms. The delayed-CP sequence shown in Fig. 1(b) was used for the selective observation of signals having long spin–spin relaxation times T_2. The contact time (t_{CP}) and the delay time (τ) were set to 0.2 and 0.5 ms, respectively.

3. Results and discussion

3.1. DSC analysis

The melting temperature (T_m) of SC film of P(VDF$_{75}$/-TrFE$_{25}$) was determined as 148 °C by DSC. Fig. 2 shows the DSC curve of SC-film on heating and cooling below T_m. An endothermic peak is observed at 125.4 °C on heating, and an exothermic peak is observed at 74.1 °C on cooling. These correspond to the transitions between the ferroelectric and paraelectric phases. The temperatures at which the phase transitions begin were determined as 118 °C on heating and 76 °C on cooling.

3.2. ^{19}F MAS NMR spectra

Fig. 3(a) shows the direct polarization (DP) ^{19}F MAS

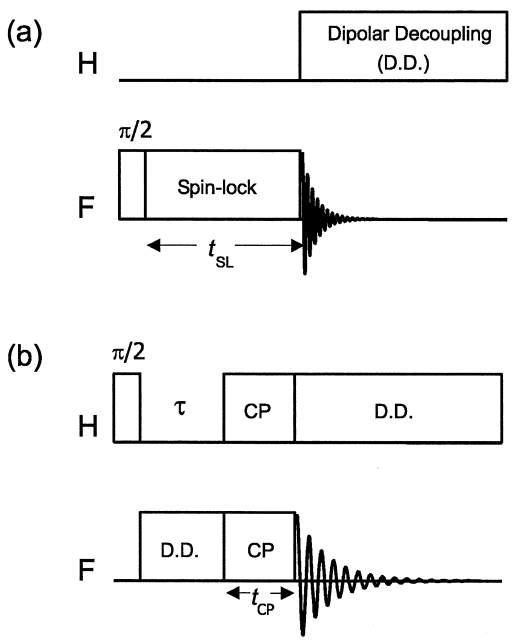

Fig. 1. Pulse sequences for (a) variable spin-lock time for $T_{1\rho}^{F}$ measurement and (b) delayed CP sequence for selective observation of domains having a relatively long T_2^H. The ordinary CP experiment was achieved without a delay time τ in the delayed CP sequence.

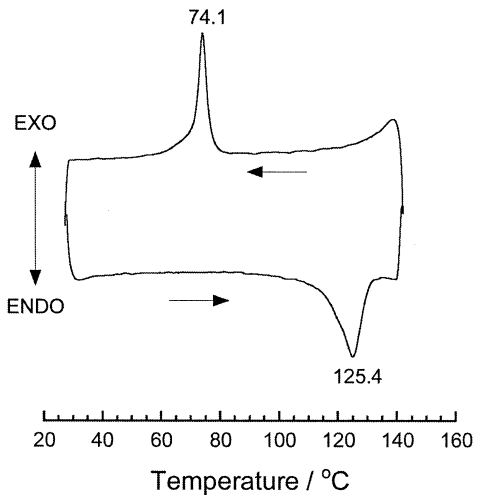

Fig. 2. DSC curve of SC-film on heating and cooling below T_m.

NMR spectra of AR-film at 68 °C with broadband ^{1}H decoupling. Seven sharp peaks are clearly observed in the spectrum, whereas only three peaks were observed in the ^{13}C CP/MAS NMR spectrum [11]. The broad component covering from −88 to −130 ppm corresponds to crystalline domains, whereas the sharp signals (peaks 1_{am} to 8_{am}) correspond to amorphous domains (see below). The latter signals were assigned according to the data from the solution-state ^{19}F NMR spectra of P(VDF/TrFE) by Mabboux and Greason [23]. The signals in the higher frequency (from −88 to −130 ppm) and the lower frequency (from −195 to −210 ppm) regions were assigned to the fluorines of CF_2 and CHF groups, respectively. Three peaks at −88.4 (peak 1_{am}), −102.2 (peak 3_{am}), and −109.2 ppm (peak 4_{am}) are assigned to the CF_2 fluorines of VDF units within different sequences. Holstein et al. [17] have reported that the amorphous signal of PVDF homopolymer is observed at $\delta_F = -91$ ppm in the

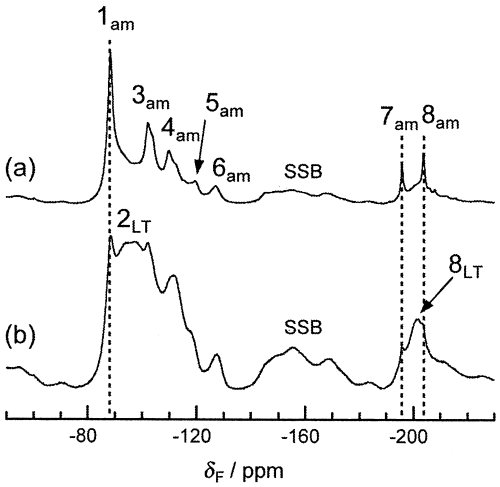

Fig. 3. Direct polarization ^{19}F MAS NMR spectra of (a) AR-film and (b) SC-film at 68 °C under a MAS rate of 16 kHz. Experimental parameters: fluorine π/2 pulse duration 2.5 μs, 32 transients, recycle delays (a) 6 and (b) 12 s, respectively.

^{19}F MAS NMR spectrum. Considering that they referred the signal of C_6F_6 as $\delta_F = -166.4$ ppm for a reference of ^{19}F chemical shifts, i.e. 2.8 ppm to lower frequency than our chemical shift reference, the δ_F of peak 1_{am} agrees well with that of the amorphous signal of PVDF homopolymer. This clearly indicates that peak 1_{am} corresponds to the CF_2 of VDF units involved in a sequence $-CF_2-CH_2-CF_2-CH_2-CF_2-$ in amorphous domains. The peaks 4_{am} to 6_{am} correspond to CF_2 fluorines adjacent to CHF groups. Peak 7_{am} at -195.8 ppm was assigned to VDF:VDF:TrFE:VDF:VDF pentamer where the VDF and TrFE units are linked by a regio-irregular *head-to-head* linkage (hereafter denoted as *H–H* linkage), i.e. $-CF_2-CH_2-CF_2-CH_2-CHF-CF_2-CF_2-CH_2-CF_2-CH_2-$ [23]. The other strong CHF peak observed at -203.7 ppm (peak 8_{am}) is assigned to the regio-regular *head-to-tail* (*H–T*) linkage of VDF:VDF:TrFE:VDF:VDF pentamer (*H–T* linkage), i.e. $-CF_2-CH_2-CF_2-CH_2-CF_2-CHF-CF_2-CH_2-CF_2-CH_2-$.

The DP ^{19}F MAS NMR spectrum of a SC-film at 68 °C is shown in Fig. 3(b). The sharp peaks with lower intensities are observed at the same chemical shifts as peaks 1_{am}, 3_{am}, and 7_{am} of AR-film. In addition, two broad but distinct signals are observed at ca. -92 and -202.0 ppm (peaks 2_{LT} and 8_{LT}), and the former is split into two peaks. As will be clarified by the crystalline-selective observation and $T_{1\rho}^F$ measurement, these peaks originate from crystalline domains. The δ_F of peak 2_{LT} agrees with the crystalline peak of the β-form of PVDF homopolymer which takes an all-*trans* conformation [17]. This is consistent with the results of X-ray diffraction studies which reported that P(VDF/TrFE) copolymers take *all-trans* conformations in the low-temperature ferroelectric phase [2,5]. Although no literature could be found for δ_F of all-*trans* TrFE sequences, peak 8_{LT} can be assigned to crystalline CHF groups of TrFE units which have all-*trans* conformation [1,2]. Reinsberg et al. [22] have reported that the isoregular CHF fluorines of PTrFE resonate at -213 ppm, while *head*-to-*head* monomer inversions give a shoulder at -219 ppm in the solid-state ^{19}F MAS NMR spectrum. No distinct peak is observed at -213 ppm in Fig. 3, indicating that TrFE units are isolated in polymer chains.

Fig. 4(a) shows the amorphous-selective spectrum of AR-film observed using the delayed-CP pulse sequence. This technique utilizes a fact that protons in the crystalline or immobile domains have a much shorter spin–spin relaxation time (T_2^H) than those in the amorphous or mobile domain. The broad crystalline peaks observed in Fig. 3(a) are effectively suppressed, and only the sharp peaks are observed. Note that the relative intensities of peaks 7_{am} and 8_{am} (CHF fluorines) in Fig. 4(a) are significantly smaller than those in Fig. 3(a). This may originate from the lower mobility of TrFE units than VDF units in the amorphous domain for AR film, though the signal intensities in the CP experiments are also affected by the efficiency of the magnetization transfer. The amorphous signals are also

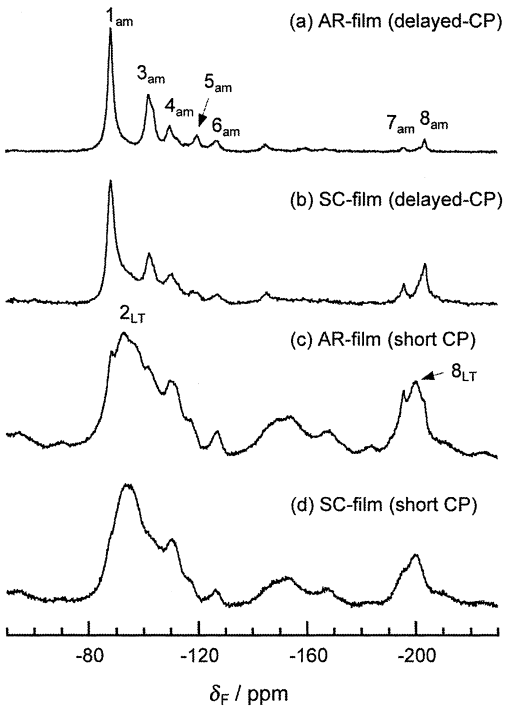

Fig. 4. Selectively observed spectra of amorphous or crystalline phases. (a) and (b) Delayed CP spectra of AR and SC films, respectively, observed with a delay time $\tau = 0.5$ ms, contact time $t_{cp} = 0.5$ ms, and 32 for (a) and 256 transients for (b). (c) and (d) $^1H \rightarrow {}^{19}F$ CP/MAS spectra with short t_{cp} (0.1 ms) of AR and SC films, respectively.

observed for a SC-film at the same δ_F as for AR-film as shown in Fig. 4(b). However, in this case the broad crystalline signals are not completely suppressed by the delayed-CP sequence, probably because of the much higher content of the crystalline domain. It should be noted that the signal intensities in Fig. 4(b) were much weaker than those in Fig. 4(a); eight times more transients were needed for the same S/N ratio for the SC-film than for the AR-film.

The $^1H \rightarrow {}^{19}F$ CP/MAS NMR spectra of AR and SC films for short contact times t_{cp} (0.1 ms) are shown in Fig. 4(c) and (d), respectively. Since the magnetization transfer from ^{1}H to ^{19}F in the crystalline domain is much more efficient than that in the amorphous domain above the glass transition temperature (T_g), the crystalline signals are selectively observed in these spectra. The broad crystalline peaks 2_{LT} and 8_{LT} are emphasized, and almost no amorphous peaks are detected for SC-film in Fig. 4(d). The spectral shapes and the chemical shifts of the characteristic peaks (2_{LT} and 8_{LT}) for AR-film coincide well with those for SC-film, indicating that the polymer chains in the crystalline domains of AR-film also take the all-*trans* conformation.

3.3. $T_{1\rho}^F$ at ambient temperature

The decays of ^{19}F magnetization for peaks 1_{am}, 7_{am}, and 8_{am} of AR-film observed by variable ^{19}F spin-lock experiments at ambient temperature (68 °C) are shown in

Fig. 5(a). The intensities are plotted using the heights of each peak instead of integrated peak areas because of the difficulty of accurate peak deconvolution. The values of $T_{1\rho}^{F}$ obtained by fitting the decays using single or double exponential functions are summarized in Table 1. The decays of all peaks for AR-film have two $T_{1\rho}^{F}$ components, in which the shorter and longer $T_{1\rho}^{F}$ components correspond to the amorphous and the crystalline domains, respectively. The two-component nature indicates that little segmental motion at around the spin-locking frequency (100 kHz) exists in the crystalline domains at 68 °C (ca. 50 °C below T_c), whereas the motion is significant in the amorphous domain. Molecular motions in the crystalline domains have been observed for fluorinated polymers such as ethylene-tetrafluoroethylene copolymer (ETFE) [27]: the phase transition in the crystalline domain of ETFE occurs over a wide temperature range (0–100 °C) even below T_g. The significant difference between the $T_{1\rho}^{F}$s of the crystalline and amorphous domains has also been observed for PVDF homopolymers [20,21]. In particular, the CF_2 signals of VDF and TrFE units (peak 1_{am}–6_{am}) exhibit shorter $T_{1\rho}^{F}$ components of ca. 1.5–1.8 ms compared with the CHF signals of TrFE units (peaks 7_{am} and 8_{am}: 3.0–4.0 ms), although the longer $T_{1\rho}^{F}$ components of the CF_2 signals of TrFE units are longer than those of the CF_2 signals of VDF units and CHF signals of TrFE units. For AR-films containing significant amounts of amorphous domains, the influence of homonuclear spin diffusion between the amorphous and crystalline domains during long spin-lock times should be considered in order to determine exact $T_{1\rho}^{F}$ values and proportions for each domain. However, the relatively large content (74%) of a short $T_{1\rho}^{F}$ component for peak 1_{am} suggest that the amorphous domains involve significant amounts of CF_2 units in the regio-regular VDF sequence. Further discussion of this point will be presented in the next paper of this series [28].

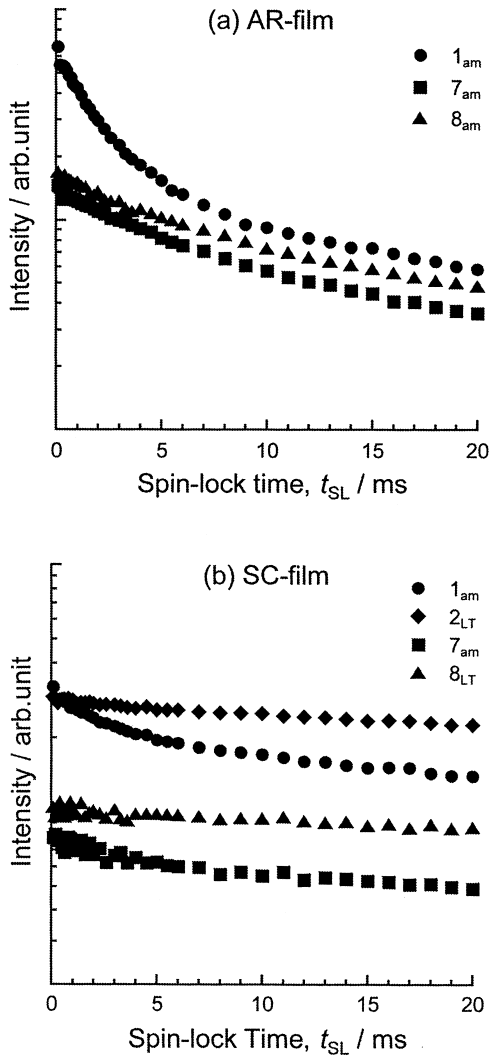

Fig. 5. Spin-lock time dependence of the ^{19}F signal intensity for (a) AR-film and (b) SC-film at 68 °C. The measured $T_{1\rho}^{F}$ values obtained using single- or double-exponential functions are summarized in Table 1.

Fig. 5(b) shows the decays of ^{19}F magnetization for peaks 1_{am}, 2_{LT}, 7_{am}, and 8_{LT} of SC-film observed by variable ^{19}F spin-lock experiments at ambient temperature. The $T_{1\rho}^{F}$ values longer than 40 ms indicate the absence of segmental motion at around 100 kHz at this temperature. The fact that the decay of peak 7_{am} (corresponding to the VDF–TrFE *H–H* linkage) exhibits a shorter $T_{1\rho}^{F}$ value compared to that of peak 8_{LT}, indicates that the segmental mobility at regio-irregular *H–H* linkages is more vigorous than that at regio-regular *H–T* linkages.

3.4. Variable temperature measurements

3.4.1. Heating process

Figs. 6(a) and 7(a) show the VT $^{1}H \rightarrow {}^{19}F$ CP/MAS NMR spectra of SC-film on heating for CF_2 and CHF fluorines, respectively. A short contact time of 0.1 ms was used for selective observation of signals from the crystalline domains. The broad crystalline peaks for CF_2 (peak 2_{LT} in Fig. 6(a)) and CHF (peaks 8_{LT} in Fig. 7(a)) regions disappeared between 115 and 119 °C, and only sharp signals were observed at 119 °C. These phenomena clearly indicate that the ferroelectric-to-paraelectric phase transition occurred in this temperature range, which agrees well with the beginning of the endotherm in the DSC chart. It should be noted that the phase transition was clearly and precisely detected by the ^{19}F MAS spectra, though no such spectral changes were observed by ^{13}C CP/MAS NMR [11]. In addition, the $T_{1\rho}^{F}$ values for all peaks rapidly decreased to ca. 20 ms above 107 °C (see below). Since peaks 1_{HT}, 7_{HT}, and 8_{HT} were assigned to VDF sequences, *H–H*, and *H–T* linkages, respectively, the decreased and unified $T_{1\rho}^{F}$ values can be explained by the vigorous *trans–gauche* exchange and the non-localized rotational motions along the polymer chains occurring in the paraelectric phase [5].

In the CF_2 region, a small shoulder is observed at −88.5 ppm at 43 °C (Fig. 6(a)), and this becomes distinguishable as a small peak (peak 1_{HT}) at 77 °C. Although the δ_F of peak 1_{HT} coincides with that of peak

Table 1
$T_{1\rho}^{F}$ values of each peak of SC and AR films obtained by fitting the decays of ^{19}F magnetization observed (see Fig. 5) by variable spin-lock experiments at 68 °C. The values in parenthesis indicate the ratio of the two components (units: ms)

Peak	1_{am}	2_{LT}	3_{am}	4_{am}	5_{am}	6_{am}	7_{am}	8_{LT}	8_{am}
δ (ppm)	−88.4	−93.8	−102.2	−110.0	−119.3	−127.1	−195.8	−201.1	−203.7
AR-film	1.7 (0.74)		1.9 (0.62)	1.5 (0.50)	1.8 (0.58)	1.8 (0.51)	4.0 (0.42)		3.0 (0.32)
	17.5 (0.26)		38.7 (0.38)	40.8 (0.50)	45.7 (0.42)	44.8 (0.49)	23.7 (0.58)		22.4 (0.68)
SC-film	2.3 (0.33)	82.6 (1.00)	2.4 (0.22)	1.9 (0.13)	1.4 (0.12)	1.5 (0.16)	41.2 (1.00)	120 (1.00)	
	51.6 (0.67)		72.9 (0.78)	75.1 (0.87)	70.5 (0.88)	63.2 (0.84)			

1_{am} (the amorphous CF_2 of VDF), the former should originate from the crystalline domain because this is clearly observed in the short-contact CP spectrum. Another distinguishable crystalline peak (7_{HT}) also appears at −196 ppm, with a larger linewidth than peak 7_{am} at 77 °C (Fig. 7(a)). At more elevated temperatures up to 115 °C, peaks 1_{HT} and 7_{HT} are gradually displaced to high frequency (to −87.2 and −194.8 ppm, respectively), whereas peak 2_{LT} resonates at the same δ_F over the range 43–115 °C. In addition, the signal intensity of peak 2_{LT} decreases in parallel with the increase in that of peak 1_{HT}. These signal displacements can be explained in terms of the changes in conformation of polymer chains. The coexistence of peaks 2_{LT} and 1_{HT} indicates that two distinct conformations for VDF chain sequences exist simultaneously; one is for an all-*trans* crystalline component and the other is for a component with a significant amount of *gauche* conformers. The latter component can be a precursor of the rotating molecules in the paraelectric phase. Similar behavior has been observed by Li et al. [29] and Tashiro et al. [30] in the X-ray diffraction patterns of the copolymer. The diffraction peak of the HT phase begins to appear with a broad half-width at temperatures ca. 30 °C lower than T_c coexisting with a relatively sharp peak of the LT phase. In contrast, only the diffraction of the HT phase with a sharper half-width was observed above T_c. The model structure for the crystalline domains proposed from the X-ray diffraction patterns agrees with our NMR observations on the coexistence of peaks 1_{HT} and 2_{LT} observed below T_c.

In contrast, no changes are observed for the peak height and δ_F for the signal of VDF–TrFE *H*–*T* linkages (peak 8_{LT}) between 43 and 92 °C (Fig. 7(a)). In addition, peak 8_{HT}, which corresponds to the paraelectric phase, newly appeared at −202.2 ppm at 99 °C, coexisting with peak 8_{LT} at −200.8 ppm. At elevated temperatures, the intensity

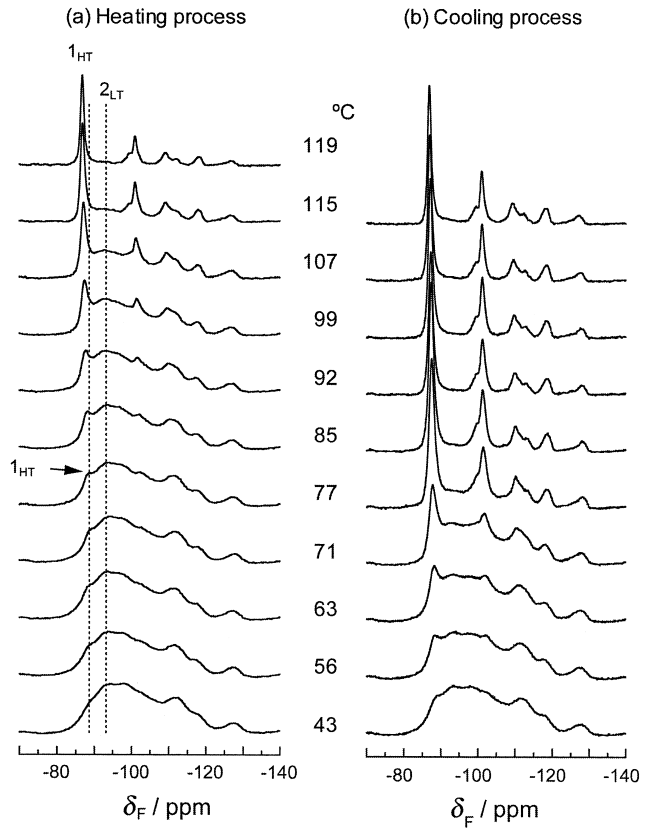

Fig. 6. Variable temperature (VT) $^1H \rightarrow {}^{19}F$ CP/MAS NMR spectra of the CF_2 region for SC-film on (a) heating and (b) cooling. Experimental parameters as in Fig. 3.

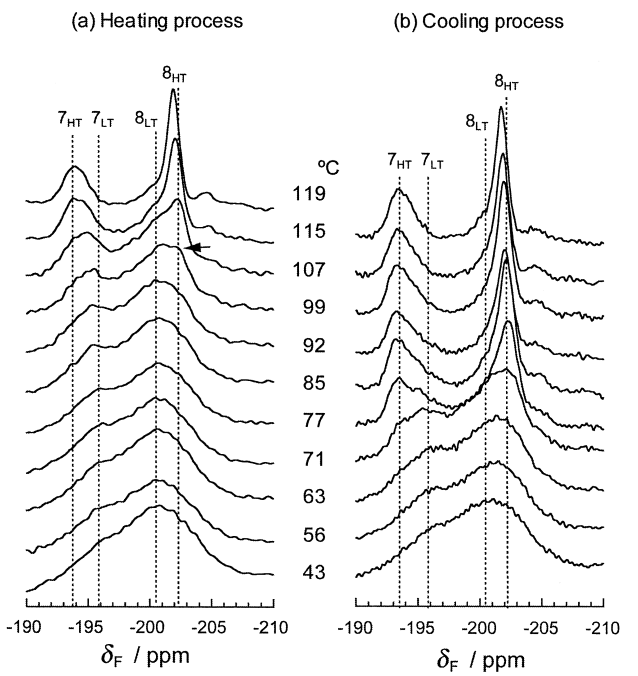

Fig. 7. VT $^1H \rightarrow {}^{19}F$ CP/MAS NMR spectra of the CHF region of SC-film on (a) heating and (b) cooling. Experimental parameters: contact time 0.1 ms, recycle delay 12 s, 32 transients.

of peak 8_{HT} gradually increased in parallel with the decrease in peak 8_{LT}. This indicates that the *trans–gauche* conformational exchange at *H–T* linkages begins at 99 °C, which is higher than that for VDF and *H–H* linkages (77 °C). In other words, *H–T* linkages are more stable than VDF and *H–H* linkages with respect to conformational exchange motion.

Fig. 8(a) and (b) shows the decays of spin-locked ^{19}F magnetization in the rotating frame below (107 °C) and above (119 °C) the phase transition, respectively, and the estimated values of $T_{1\rho}^{F}$ are summarized in Table 2. The values of $T_{1\rho}^{F}$ longer than 40 ms, which are observed for all peaks at 107 °C, indicate that there is little molecular mobility at around the spin-locking frequency in the crystalline domain even near T_c. In addition, the fact that $T_{1\rho}^{F}$ of peak 7_{HT} is shorter than that of peak 8_{HT} suggests that the *H–H* linkage has higher mobility than the *H–T* linkage,

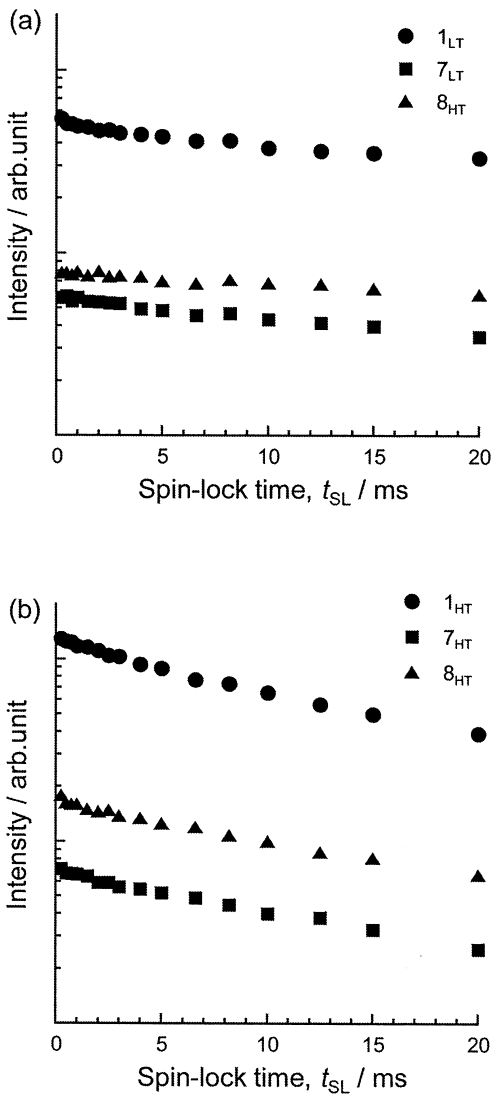

Fig. 8. Spin-lock time dependence of the ^{19}F signal intensity measured (a) before (107 °C) and (b) after (119 °C) the phase-transition temperature on heating.

Table 2
$T_{1\rho}^{F}$ values of each peak of the SC-film obtained by fitting the decays of ^{19}F magnetization observed by variable spin-lock experiments on heating and cooling (units: ms)

Temperature/°C	1_{HT}	3	4	5	6	7_{HT}	8_{HT}	
Heating	107	55	114	94	37	48	39	73
	119	21.6	22.0	20.0	20.2	19.2	21.9	21.3
Cooling	85	16.4	20.1	18.9	20.8	12.9	13.9	14.4
	77	28	36	42	54	53	43	33

which coincides with the observation that peak 8_{HT} only appears 22 °C higher than peak 7_{HT}. Further, the $T_{1\rho}^{F}$ of all peaks, both in the crystalline and amorphous domains, abruptly collapsed to a unique value of ca. 20 ms at 119 °C. These identical $T_{1\rho}^{F}$ values above T_c indicate that uniform molecular motion including all chain sequences then occurs. This clearly shows that the polymer chains both in the crystalline and amorphous domains were involved in the phase transition, accompanied by uniform and vigorous molecular motion. It has been proposed that the molecular chains rotate around the chain axis in the paraelectric phase [2,4,5]. The significant variations observed for $T_{1\rho}^{F}$ during the establishment of the paraelectric phase are consistent with this view motional model.

The temperature dependence of the ^{19}F spin–lattice relaxation time, T_1^F, on heating is shown in Fig. 9. With increasing temperature, the T_1^F values gradually decrease, suggesting that localized molecular motion such as vigorous oscillation or flip-flop reorientation at rates of around several hundred MHz increases at elevated temperatures. Ishii et al. [8–10] have analyzed the behavior of T_1^H for P(VDF/TrFE) with VDF contents of 52–72% and concluded that flip-flop motion of TrFE units between two sites 180° apart occurs between 30 and 80 °C, and that this motion changes to a hindered rotational motion near T_c. In

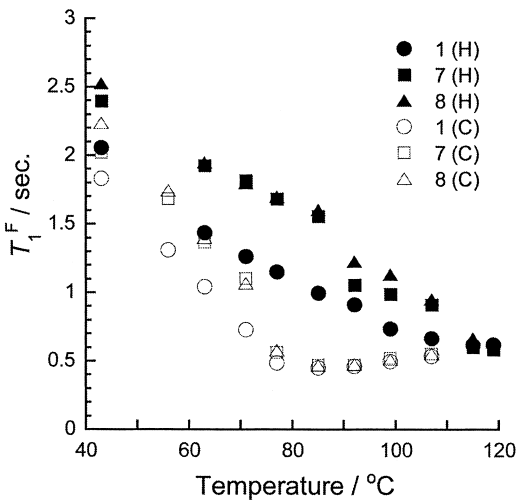

Fig. 9. Temperature dependence of the spin–lattice relaxation time T_1^F for SC-film. Filled and open symbols represent heating (H) and cooling (C), respectively.

addition, the oscillation motion of VDF segments with an amplitude of 10°, which is estimated from the analysis of the NMR second moment, occurs between 80 and 114 °C [8]. The gradual decrease in T_1^F observed in the present study at 43–107 °C agrees with the increase in flip-flop and/or oscillation motion. In addition, the significant displacements of peaks 1_{HT} and 7_{HT} to higher frequency with increasing temperature indicate that local conformational exchange also occurs, accompanying the flip-flop and/or oscillation motion [5].

The conformational exchange occurring between *trans* and *gauche* conformers at the CF_2 of VDF units can be inferred from the chemical shift of peak 1_{HT}. As has been reported by Holstein et al. [17] and the present authors [24], two distinct crystalline peaks are observed at −79 and −95 ppm for the α-crystalline phase of PVDF homopolymer, whilst a single peak is observed at −95 ppm for the β-crystalline phase. The polymer chains take TG^+TG^- and all-*trans* (TTTT) conformations, respectively. In addition, a sharp signal of amorphous domains is always observed at −88.6 ppm. This resonant position can be explained by significant molecular motion that averages the chemical shifts, reflecting the differences in conformations and stereochemical structures within the NMR timescale [17]. If fast molecular motion occurs for all-*trans* conformers (β-crystalline phase) and thus similar amounts of *trans* and *gauche* conformers are generated, the resulting signal should resonate at −87 ppm (at the center of the two crystalline peaks of the α-crystalline phase). This means that an increase of *gauche* conformers causes a displacement to higher frequency for the average chemical shift of CF_2 fluorines. In addition, an increase of the Raman intensity of the *gauche* band for $P(VDF_{73}/TrFE_{27})$ copolymer was found at ca. 80 °C [31]. This temperature agrees well with the temperature at which the higher frequency shift of peak 1_{HT} begins (77 °C in Fig. 6(a)). Hence, the shift of peak 1_{HT} can be explained by an increase in *gauche* conformers originating from the localized conformational exchange motion, which was also detected by the decrease in T_1^F. In addition, *trans* conformers are more dominant than *gauche* conformers at the regio-regular VDF units in the amorphous phases because their chemical shift (−88.6 ppm) is closer to the δ_F of all-*trans* conformations for both PVDF and P(VDF/TrFE).

In a similar manner, peak 7_{HT} is displaced to higher frequency at elevated temperatures from 43 to 92 °C, whereas peak 8_{LT} shows no displacement (Fig. 7(a)). Moreover, peak 8_{HT}, which newly appears at 99 °C, increases its intensity through the phase-transition temperature range. These facts indicate that the conformational exchange at sequential VDF units and VDF–TrFE *H*–*H* linkages become gradually more vigorous between 77 and 119 °C, whereas the *trans*–*zigzag* conformations at VDF–TrFE *H*–*T* linkages are fixed between 43 and 92 °C. In the paraelectric phase at 119 °C, peak 8_{HT} is shifted to higher frequency by 0.4 ppm from its value at 107 °C. This can be explained by an increase in *trans* conformers in the paraelectric phase. Ishii et al. [11] have suggested from ^{13}C CP/MAS experiments that TrFE-rich segments do not transform to *gauche* conformers in the paraelectric phase. However, as seen in our ^{19}F spectra, peaks 7_{HT} and 8_{HT} exhibited significant displacements to higher and lower frequency, respectively, indicating that the substantial conformational changes occur at the TrFE units. The amount of *trans* conformers at the *H*–*T* linkages, however, increases in the paraelectric phase, as observed by the shift of peak 8_{HT} to higher frequency between 115 and 119 °C, closer to the chemical shift of the all-*trans* conformer (peak 8_{LT}). This suggests that the *trans* conformer at the *H*–*T* linkage is more stable than at the *H*–*H* linkage in the paraelectric phase.

We can summarize the phase transition behavior on heating as follows. Conformational exchange between *trans* and *gauche* conformers of main chains gradually becomes more vigorous at VDF units and *H*–*H* linkages between 43 and 92 °C, whereas no such exchange occurs at *H*–*T* linkages. At 92 °C, the exchange motion begins also for *H*–*T* linkages, and the *trans*–*gauche* exchange of VDF chains promptly enhances the cooperative motion with *H*–*T* linkages at elevated temperatures from 92 to 115 °C. The *H*–*T* linkage is supposed to act as an anchor that prevents the molecular chains from entire and simultaneous chain rotations. Therefore, we consider that the *H*–*T* linkage in VDF–TrFE sequence plays a key role in the ferroelectric-to-paraelectric phase transition. The rotational motion around the chain axis promptly begins between 107 and 119 °C. In the paraelectric phase above T_c, *H*–*T* linkages includes more *trans*-rich conformers in rotational motion than the sequential VDF units and *H*–*H* linkages.

3.4.2. Cooling process

The VT $^1H \rightarrow {}^{19}F$ CP/MAS NMR spectra of SC-film during the cooling process are shown in Figs. 6(b) and 7(b). There is no significant change in the spectral shapes between 119 and 85 °C except for slight signal displacements of peaks 1_{HT}, 7_{HT}, and 8_{HT} to lower frequency. However, the crystalline signals, peaks 2_{LT} and 8_{LT}, abruptly appeared at 77 °C, indicating that the paraelectric to ferroelectric phase transition occurred between 85 and 77 °C on cooling. This temperature range agrees well with T_c during cooling (76 °C) measured by DSC. At lower temperatures, the intensities of the sharp signals decreased, and those of the crystalline signals increased complementarily. Small shoulders, which are the remnants of sharp components, are still observed at 43 °C, while no such shoulder is observed at the same temperature on heating (Figs. 6(a) and 7(a)). This means that the conformational exchange motion was not completely frozen at 43 °C on cooling, which differs from the heating process. Fig. 10 shows a magnification of the VDF part of Fig. 6(b). The shift of peak 1_{HT} to lower frequency is observed between 115 and 85 °C even in the paraelectric phase, suggesting a decrease

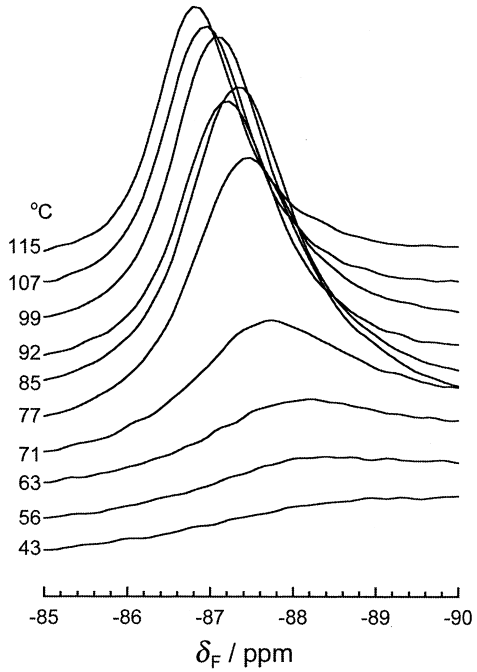

Fig. 10. Magnification of the VDF region of VT $^1H \rightarrow {}^{19}F$ CP/MAS NMR spectra for SC-film on cooling.

in the proportion of *gauche* conformers in VDF sequences. Peak 8_{HT} is also displaced to lower frequency (Fig. 7(b)) in the same temperature range. In contrast to peak 1_{HT}, the displacement of peak 8_{HT} implies an increase in *gauche* conformers at $H-T$ linkages. These changes can be understood as *trans* conformer increases at VDF units with lowing temperature toward T_c, with increase of *gauche* conformers at the $H-T$ linkages in cooperation with the motion at VDF sequences. Below the transition temperature, the exchange motion promptly slows down and *gauche* conformers revert to more stable *trans* ones.

The $T_{1\rho}^F$ values above (85 °C) and below (77 °C) the phase transition are summarized in Table 2. The $T_{1\rho}^F$ of peaks 1_{HT}, 7_{HT}, and 8_{HT} slightly decrease from 22 ms (119 °C) to 14–16 ms (85 °C), and the minima are found at 85 °C. At lower temperatures below T_c, $T_{1\rho}^F$ values return to the longer values that were observed before heating. Ishii et al. [11] have also found minima of $T_{1\rho}^H$ detected by ^{13}C signals of CH_2 and CF_2 in the same temperature range, though no change was found for the $T_{1\rho}^H$ detected by CHF carbon signals. Hence, they concluded that the *trans* conformation of TrFE units does not change through the phase transition, although the segments are in vigorous motion. However, the signal displacements of peaks 7_{HT} and 8_{HT} and the $T_{1\rho}^F$ minimum observed at T_c for the ^{19}F signal of CHF units clearly indicate that conformational changes take place at TrFE units.

The temperature dependence of T_1^F on cooling is shown in Fig. 9. The values of T_1^F for all peaks are identical in the paraelectric phase, and they tend to decrease in the range 107–85 °C. Note that a minimum of T_1^F is found at around T_c during cooling (85 °C). This clearly indicates that $T_{1\rho}^F$ is sensitive to the molecular motion caused by the phase transition. At 77 °C, below T_c, T_1^F for each peak starts to have different values, and they increase with lowering temperature. On further lowering of the temperature, T_1^F increases and becomes close to the initial value for the heating process, but is still shorter at 43 °C than that at 43 °C on heating. This suggests that the conformational exchange motion still exists near ambient temperature on cooling.

3.4.3. Comparison between the amorphous and paraelectric phases

At first sight, the spectral shape for the paraelectric phase of SC-film at 119 °C (Figs. 6(a) and 7(a)) and that of the amorphous phase of AR-film at 68 °C (Fig. 4(a)) are similar. However, some significant differences are found in the chemical shifts and molecular mobility. The peak 1_{HT} in the paraelectric phase is at −86.9 ppm, whereas that in the amorphous phase is observed at −88.4 ppm. High-frequency displacements caused by phase transition are also observed for the other peaks (except for peak 6). As mentioned above, these shifts can be ascribed to the variations in the content of *gauche* conformers. VT ^{19}F MAS spectra reveal that *trans* conformers are dominant in the amorphous domain, whereas *trans* and *gauche* conformers exist almost equally for sequential VDF units in the paraelectric phase as shown by peak 1_{HT} in the paraelectric phase being observed at the central position of the two crystalline peaks of the α-form of PVDF. In addition, a large difference should exist in molecular mobility between these phases. The $T_{1\rho}^F$ values for the amorphous phase is 2–3 ms for all peaks (Fig. 5 and Table 1), whereas those for paraelectric phase are ca. 20 ms. This can be interpreted as that vigorous and random motion occurs in the amorphous phase, while rotational motion along the polymer chains uniformly occurs in the paraelectric phase. In the latter phase, the molecular chains can rotate almost freely around the chain axis, but the chains are hindered from moving in the direction perpendicular to the chain axis because each chain is restricted to a cylindrical cavern [12]. The observed longer $T_{1\rho}^F$ (ca. 20 ms) in the paraelectric phase (compared with those in the amorphous phase) should be related to this restricted motion in the paraelectric phase.

4. Conclusions

The phase structure and molecular mobility of P(VDF_{75}/-$TrFE_{25}$) have been analyzed using solid-state ^{19}F MAS and $^1H \rightarrow {}^{19}F$ CP/MAS NMR. The sharp peaks, which correspond to amorphous domains, are observed together with broad crystalline signals in the direct polarization ^{19}F MAS NMR spectrum with broadband ^1H decoupling of AR-film. Significant differences in $T_{1\rho}^F$ between the crystalline and amorphous domains at 68 °C are confirmed by spin-lock experiments. The phase-transition behavior is followed by

variable temperature $^{1}H \rightarrow {}^{19}F$ CP/MAS measurements for short contact times for selective observation of crystalline domains. With increasing temperature, the signal for VDF chain sequences is displaced to higher frequency by 1.6 ppm, with gradual decrease of its T_1^F. This indicates that fast and local conformational exchange between *trans* and *gauche* conformers increases at elevated temperature. The signal displacements are observed not only for VDF chain sequences but also for TrFE units, indicating that conformational changes occur through the chain sequences, which differs from the result of ^{13}C CP/MAS NMR. The exchange motion occurs increasingly in VDF chain sequences and at *H–H* linkages between 77 and 115 °C, whereas that at *H–T* linkages begins above 92 °C and increases up to 115 °C. This means that the *H–T* linkage stabilizes the *trans* chains, preventing full chain rotation in the ferroelectric phase. The phase transition can be easily detected by the disappearance of the broad all-*trans* crystalline signals in ^{19}F MAS spectra. The fact that the $T_{1\rho}^F$ values for all peaks decrease to similar values between 115 and 119 °C is strong evidence for the rotational motion around the chain axis in the paraelectric phase. In addition, the proportion of *gauche* conformers at VDF chain sequences in the paraelectric phase is higher than that in the amorphous phase, which is confirmed by a higher frequency shift by 1.6 ppm. In addition, the significantly longer $T_{1\rho}^F$ in the paraelectric phase compared to those in amorphous domains indicates that polymer chains undergo anisotropic rotational motion around the chain axis in the paraelectric phase, while they undergo vigorous isotropic motion in amorphous domains. For the cooling process, the signal displacements indicate that the proportion of *trans* conformers gradually increases at VDF chain sequences, whereas that of *gauche* conformers increases at TrFE units. The phase transition temperature observed by ^{19}F MAS spectra on cooling agrees well with the T_c observed by DSC.

Acknowledgements

We wish to thank Y. Tanaka, M. Sato, and E. Fujita at Daikin Industries, Ltd for providing P(VDF_{75}/$TrFE_{25}$) copolymer. We are grateful to D.C. Apperley, P. Hazendonk and P. Wormald for help with measurements and discussions.

References

[1] Furukawa T. Phase Transitions 1989;18:143.
[2] Tashiro K. In: Nalwa HS, editor. Ferroelectric polymers. New York: Marcel Dekker; 1995. Chapter 2.
[3] Ohigashi H, Omote K, Gomyo T. Appl Phys Lett 1995;66:3281.
[4] Tashiro K, Takano K, Kobayashi M, Chatani Y, Tadokoro H. Polymer 1984;25:195.
[5] Tashiro K, Takano K, Kobayashi M, Chatani Y, Tadokoro H. Ferroelectrics 1984;57:297.
[6] Tanaka R, Tashiro K, Kobayashi M. Polymer 1999;40:3855.
[7] Abe Y, Tashiro K. Polymer 2001;42:3409.
[8] Ishii F, Odajima A, Ohigashi H. Polym J 1983;15:875.
[9] Ishii F, Odajima A. Polym J 1986;18:539.
[10] Ishii F, Odajima A. Polym J 1986;18:547.
[11] Ishii F, Ohga F, Tsutsumi A, Ohigashi H. J Polym Sci Polym Phys 2002;40:1026.
[12] Ohigashi H, Omote K, Abe H, Koga K. J Phys Soc Jpn 1999;68:1824.
[13] Harris RK, Jackson P. Chem Rev 1991;91:1427.
[14] Ando S, Harris RK, Scheler U. In: Grant DM, Harris RK, editors. Encyclopedia of nuclear magnetic resonance, vol. 9. Chichester: Wiley; 2002. p. 531–50.
[15] Scheler U, Harris RK. Solid State Nucl Magn Reson 1996;7:11.
[16] Holstein P, Scheler U, Harris RK. Magn Reson Chem 1997;35:647.
[17] Holstein P, Scheler U, Harris RK. Polymer 1998;39:4937.
[18] Holstein P, Harris RK, Say BJ. Solid State Nucl Magn Reson 1997;8:201.
[19] Ando S, Harris RK, Holstein P, Reinsberg SA, Yamauchi K. Polymer 2001;42:8137.
[20] Ando S, Harris RK, Reinsberg SA. Magn Reson Chem 2002;49:97.
[21] Wormald P, Apperley SC, Beaume F, Harris RK. Polymer 2003;44:643.
[22] Reinsberg SA, Ando S, Harris RK. Polymer 2000;41:3729.
[23] Mabboux PY, Gleason KK. J Fluorine Chem 2002;113:27.
[24] Ando S, Harris RK, Monti GA, Reinsberg SA. Magn Reson Chem 1999;37:709.
[25] Aliev AE, Harris KDM. Magn Reson Chem 1994;32:366.
[26] Bloch F, Siegert A. Phys Rev 1940;57:522.
[27] Tanigami T, Yamaura K, Matsuzawa S. Polymer 1986;27:1521.
[28] Aimi K, Ando S. Polymer (second article of this series).
[29] Li GR, Kagami N, Ohigashi H. J Appl Phys 1992;72:1056.
[30] Tashiro K, Tanaka R, Ushitora K, Kobayashi M. Ferroelectrics 1995;171:145.
[31] Tashiro K, Kobayashi M. Polymer 1988;29:426.